J Mater Sci (2009) 44:5113–5119
DOI 10.1007/s10853-009-3503-y

FERROELECTRICS

Strain-induced artificial multiferroicity in $Pb(Zr_{0.53}Ti_{0.47})O_3$/$Pb(Fe_{0.66}W_{0.33})O_3$ layered nanostructure at ambient temperature

Ashok Kumar · R. S. Katiyar · Ramesh Nath Premnath · Carlos Rinaldi · J. F. Scott

Received: 4 March 2009 / Accepted: 17 April 2009 / Published online: 19 May 2009

Abstract Layered nanostructures (LNs) of the commercial ferroelectric $Pb(Zr_{0.53}Ti_{0.47})O_3$ (PZT) and the natural ferroic relaxor $Pb(Fe_{0.66}W_{0.33})O_3$ (PFW) were fabricated with a periodicity of PZT/PFW/PZT (~5/1/5 nm, thickness ~250 nm) on MgO substrates by pulsed laser deposition. The dielectric behavior of these LNs were investigated over a wide range of temperatures and frequencies, observing Debye-type relaxation with marked deviation at elevated temperatures (>400 K). High dielectric constant and very low dielectric loss were observed below 100 kHz and 400 K, whereas the dielectric constant decreases and loss increases with increase in frequency, similar to relaxor ferroelectrics. Asymmetric ferroelectric hysteresis loops across UP and DOWN electric field were observed with high remanent polarization (P_r) of about 33 μC/cm^2. High imprint (~5–7 V across 250 nm thin films) were seen in ferroelectric hysteresis that may be due to charge accumulation at the interface of layers or significant amount of strain (~3.21) across the layers. Room temperature ferromagnetic hysteresis was observed with remanent magnetization 5.32 emu/cc and a coercive field of ~550 Oe. Temperature and field dependent leakage current densities showed very low leakage ~10^{-7}–10^{-5} A/cm^2 over 500 kV/cm. We observed imprint in hysteresis that may be due to charge accumulation at the interface of layers or active role of polar nano regions (PNRs) situated in the PFW regions.

A. Kumar · R. S. Katiyar (✉)
Department of Physics and Institute for Functional Nanomaterials, University of Puerto Rico, San Juan, PR 00931-3343, USA
e-mail: rkatiyar@uprrp.edu

R. N. Premnath
Argonne National Laboratory, 9700 South Cass Ave, Argonne, IL 60439, USA

C. Rinaldi
Department of Chemical Engineering and Institute for Functional Nanomaterials, University of Puerto Rico, Mayagüez, PR 00681-9046, USA

J. F. Scott (✉)
Department of Earth Sciences, University of Cambridge, Cambridge CB2 3EQ, UK
e-mail: jsco99@esc.cam.ac.uk

Introduction

The lack of single phase multiferroics and increasing awareness of fabrication of magnetoelectric multiferroic materials at ambient temperature have led to renewed interest in exploring the fabrication of alternating ferroelectric/ferromagnetic layered nanostructures (LNs) [1–7]. We adopted a different approach which led us to pursue the fabrication of alternating commercially used ferroelectric $Pb(Zr_{0.53}Ti_{0.47})O_3$ (PZT) and natural multiferroic relaxors $Pb(Fe_{0.66}W_{0.33})O_3$ (PFW) in layered nanostructures. These nanostructures have more than one ferroic property and because of the coupling among magnetic, elastic, and electric polarizations, give rise to new physical phenomena and applications [1–3]. One thing that should be noticed is that PZT/PFW layered nanostructures have an extra degree of freedom, i.e., the existence of multiferroic polar nano regions (PNRs) similar to the recent discoveries of magnetoelectric relaxors and magnetic control of large polarization [8, 9].

There are only a few single phase materials existing in nature which have multiferroic properties at ambient

conditions, i.e., $Pb(Fe_{0.66}W_{0.33})_{0.80}Ti_{0.20}O_3$ [10], $PbFe_{1/2}Nb_{1/2}O_3$ [11] and $BiFeO_3$ (BFO) [4]. In order to compensate the deficiencies of natural multiferroics, alternate methods have been employed, such as nanocomposites, multilayers, superlattices, etc. These are comprised of a mixture of two different types of materials with separate or combined ferromagnetic and ferroelectric properties. From theoretical considerations of magnetoelectric (ME) effects in composites, a strong ME effect could be realized in a composite consisting of magnetostrictive and piezoelectric phases, in which the mechanical deformation due to magnetostriction results in dielectric polarization due to the piezoelectric effect.

Nanostructures provide extra degrees of freedom to design enhanced magnetoelectric multiferroics and better ME coupling which can be modulated at the nanoscale with proper tuning of the physical properties/parameters of each separate entity [12]. Several nanostructured thin film forms have been reported, among them a few are listed here: heterostructures of $BaTiO_3$ (BTO)-CFO [13], nanocomposites of BFO-CFO [14], superlattices of $La_{0.6}Sr_{0.4}MnO_3$/$0.7Pb(Mg_{1/3}Nb_{2/3})O_3$-$0.3PbTiO_3$ [15], multilayers of BFO/$Pb(Zr_{0.5}Ti_{0.5})O_3$ [16], and layered nanostructured thin films [5, 6]. However the basic physics of these nanostructures, needed for development of proper device applications, is lacking.

In the present study epitaxial PZT/PFW layered nanostructures (LNs) with alternating layers of PZT ~5 nm and PFW ~1 nm were fabricated on a MgO substrate with $La_{0.5}Sr_{0.5}CoO_3$ (LSCO) as the bottom conducting electrode by using the pulsed laser deposition technique. PZT/PFW LNs have ferroelectric and multirelaxor (birelaxor) properties at room temperature. For the first time, we have fabricated the PZT/PFW LNs and measured the temperature and frequency dependence of their ferromagnetic, ferroelectric, and electrical properties. Unique features were observed, such as a colossal (~5–7 V) imprint in ferroelectric hysteresis that is not due to lattice mismatch between substrate and films but due to the electrostatic strain/lattice mismatch between ferroelectric and multirelaxor layers. Since the ferroelectric layers are sandwiched between two multirelaxor (PFW) layers as shown in the sketch diagram (Fig. 1), their imprints were observed in the positive and negative side under application of external "up" and "down" electric fields respectively. In the case of imprint due to substrate and films, imprints on only one polarity have been observed which shift a little to the opposite polarity under application of a "down" electric field [17–19]. High dielectric constant, low tangent loss at lower frequencies and low dielectric constant, high tangent loss at higher frequencies were observed respectively. Similar phenomena have been observed in epitaxial ferroelectric heterostructures [20]. We also report the existence of polar nano-regions (PNRs) along with switchable polarization in LNs.

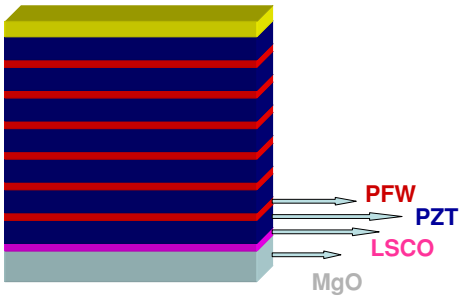

Fig. 1 Schematic of PZT/PFW layered nanostructure with LSCO as conducting bottom electrode on MgO substrate

Experimental

Layered nanostructures (LN) of Ferroelectric $Pb(Zr_{0.53}Ti_{0.47})O_3$ (PZT) and multiferroic relaxor $Pb(Fe_{0.66}W_{0.33})O_3$ (PFW) with alternate layers of PZT ~5 nm and PFW ~1 nm were deposited from individual PZT and PFW targets on conducting (bottom electrode) $LaSr_{0.5}Co_{0.5}O_3$ (LSCO) ~80 nm layer on MgO substrate using pulsed laser deposition with total thickness of LN films ~250 nm. PZT and PFW ceramic targets of 2 cm diameter were prepared by conventional solid-state route. An excimer laser (KrF, 248 nm) with a laser energy density of 1.5 J/cm^2 and pulse repetition rate of 10 Hz was used to deposit the LN films. During deposition the substrate temperature was maintained at 600 °C and oxygen pressure of 200 mTorr. The LSCO was deposited at 600 °C and oxygen pressure of 300 mTorr. The films were characterized by X-ray diffraction (XRD) using Cu K_α radiation in a Siemens D500 difractometer and the surface morphology of the films was investigated by AFM in contact mode over a 5 × 5 μm area and 20 nm heights. For electrical measurements, capacitors were fabricated by sputtering Pt top electrodes with a diameter of ~200 μm through a shadow mask. Note that values of dielectric constant ε and polarization P quoted in this paper assume the electrode diameters are the same as the diameter of the mask holes; due to Pt diffusion, this gives an overestimate of both ε and P. The dielectric properties in the frequency range of 100 Hz to 1 MHz were studied using an impedance analyzer (HP4294A from Agilent Technology Inc.) over a wide temperature range (100–650 K) attached to a temperature controlled probe station (MMR Technology) with an accuracy of ±0.5 °C. Magnetic measurements were carried out using a Quantum Design MPMS XL-7 SQUID magnetometer. The sample was placed in a standard drinking straw sample holder and the sample space was evacuated

multiple times to ensure removal of air by displacing it with He. The hysteresis curves were measured at room temperature under applied fields of up to 7 T. Magnetic measurements were carried out parallel to the c-axis (i.e. applied field was perpendicular to the substrate).

Results and discussion

Figure 2a shows the X-ray diffraction (XRD) pattern of PZT/PFW epitaxial LNs thin film. The films were found to be epitaxial with a small $\sim 0.01\%$ intensity of the (110) peak. These are oriented with an in-plane epitaxial relationship LNs [100] ‖ LSCO [100] ‖ MgO [100]. The room temperature lattice parameters of LNs, LSCO, PZT and PFW are given in Table 1. The lattice mismatch (ε) between substrate/bottom electrodes/PZT/PFW are calculated from the equation $\varepsilon = [(a_{substrate} - a_{film})/(a_{substrate})] \times 100\%$ and are listed in Table 1. We observed a tensile strain ($\sim 1.60\%$) between substrate/LNs and compressive strain ($\sim -5.24\%$) between bottom electrode/LNs along the c-axis, so we cannot exactly determine the exact nature of the depth dependence of strain on the LNs. We also believe that there were negligible effects of these strains on imprint in ferroelectric hysteresis (discussed later), since under the same conditions (substrate, bottom electrode) we grew pure PZT and did not observe any imprint in ferroelectric hysteresis. This suggests imprint somehow arises from the lattice mismatch across the interfaces of PZT/PFW/PZT. Strain across the interfaces of PZT/PFW were examined which revealed that a tensile strain of $\sim 3.11\%$ along the c-axis occurs during UP polarization whereas a compressive strain of $\sim -3.21\%$ along c-axis occurs during DOWN polarization. These calculations confirm and support the +Ve and −Ve shift of ferroelectric hysteresis from the origin during UP and DOWN applied electric fields. Below we will use these strain data to explain the imprint in ferroelectric hysteresis. Misfit strain is not the only possible source of strain in the LNs. Strain due to thermal stress arose in the film because MgO, LSCO, PZT, and PFW have different thermal expansion coefficients and are constrained to contract at the same rate on cooling. The surface morphology of the films was investigated by AFM in contact mode over a 5 × 5 μm area and 20 nm heights, as shown in Fig. 2b. Well-defined grains with dimensions ~ 10 nm in height and 180 nm width were observed. Surface topography revealed average surface roughness of 2.021 nm. The observed smaller grain size and low surface roughness may be due to growth at moderate temperature and utilization of the pulse laser deposition technique. The piezo-force microscopy (PFM) image showed the dark and bright contrast which indicates the difference in domain orientation and the presence of these nano-domains (not shown here). Interestingly, when the amplitude and phase images are compared, the regions of the nano-domains which appear dark in the phase image are also the regions with higher piezoresponse (bright regions) in the amplitude data.

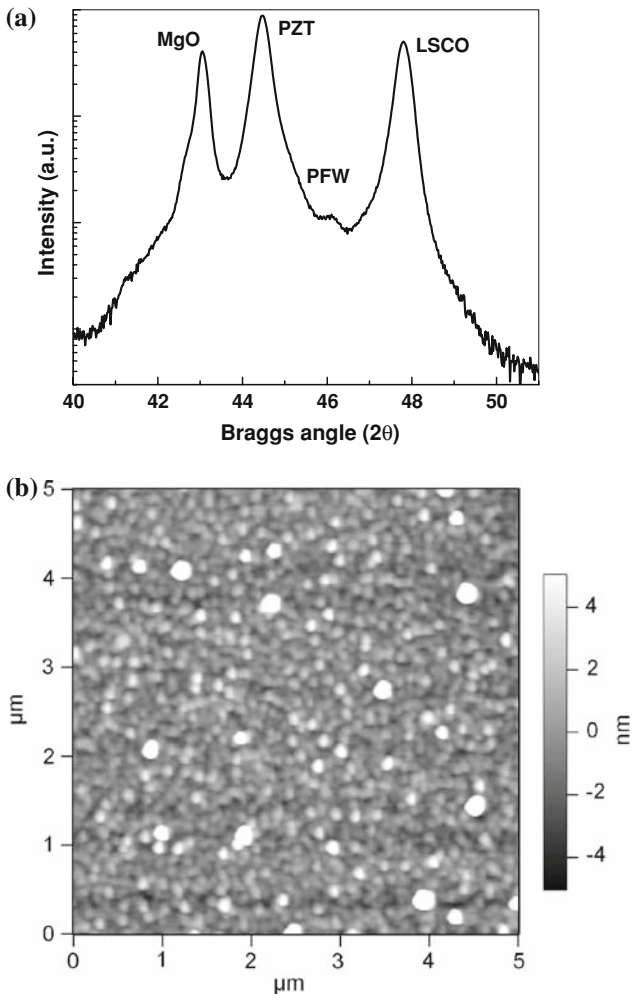

Fig. 2 **a** Room temperature XRD patterns of PZT/PFW LNs showing epitaxial nature of films. **b** Surface morphology of the LNs thin films by AFM in contact mode over a 5 × 5 μm area and 20 nm heights

Figure 3a and b show the real (ε') and imaginary (ε'') part of dielectric permittivity as function of frequency at several temperatures (100 K to 500 K). Step like behavior was observed in (ε') at 50–250 kHz from 100 to 500 K, at the same diverging frequencies dielectric loss ε'' peaks occur suggesting Debye type relaxation. The frequency dependence of ε'' showed a Debye-like relaxation peak which shifted to higher frequencies with increasing temperature. The frequency dependence of ε'' can be represented by the empirical Cole–Cole relaxation equation [21]

$$\varepsilon^*(\omega) = \varepsilon'(\omega) - i\varepsilon(\omega) = \varepsilon_\infty + \frac{(\varepsilon_0 - \varepsilon_\infty)}{1 + (i\omega\tau_0)^{1-\alpha}}, \quad (1)$$

Table 1 Lattice mismatches and their strain in epitaxial layered nanostructure thin films

Substrate/ sublayer	Lattice parameter (Å)	Lattice mismatch (%) with LSCO	Lattice mismatch (%) with PZT	Lattice mismatch (%) with PFW
MgO rocksalt	4.213	8.97	4.20	4.65
			1.60	
LSCO cubic	3.835	–	−5.24	−4.74
			−8.10	
PFW multi relaxors	4.017	–	−0.472	–
			−3.21	
PZT tetragonal	4.036	–	–	0.47
	4.146			3.11

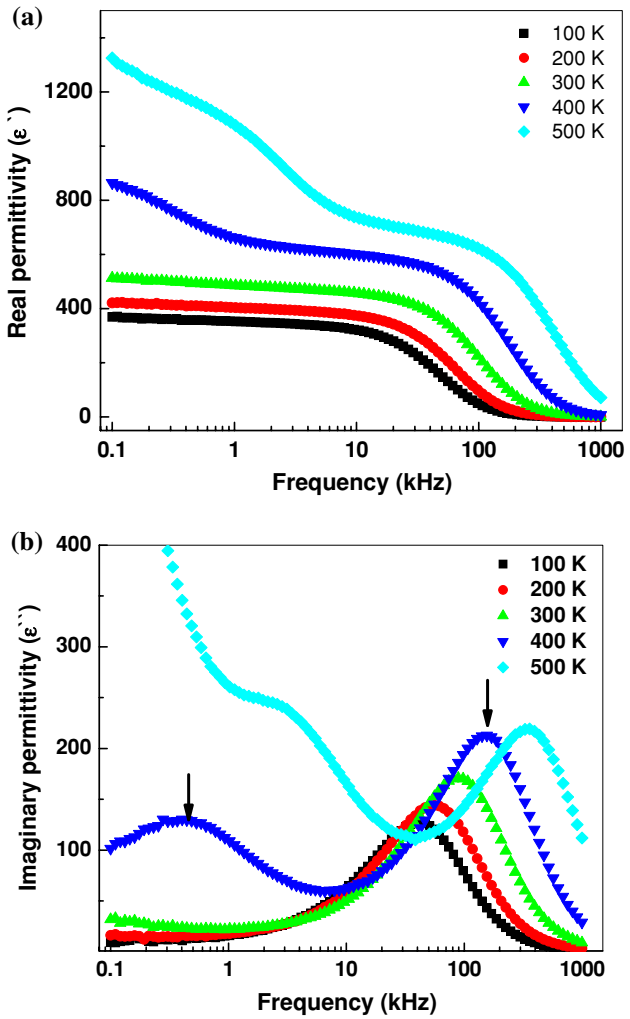

Fig. 3 **a** and **b** Real and imaginary part of permittivity as functions of frequency from 100 to 500 K

where ω is the frequency of the applied electric field (10^2–10^6 Hz), ε_0 and ε_∞ are the static and high frequency limit of the dielectric constant, τ_0 is the most probable relaxation time, and α is a constant with values between 0 and 1. For $\alpha = 0$, Eq. 1 reduces to the Debye expression. When $\alpha > 0$, the relaxation has a distribution of relaxation times, leading to a broader peak than the Debye peak. Our Cole–Cole fitting of dielectric loss spectra indicated nearly ideal Debye relaxation. The α value increased with temperature, suggesting that the distribution of relaxation times narrowed with temperature. One more relaxation at low frequency were observed at elevated temperatures (>400 K) which shifted to higher frequency with increasing temperature suggesting these are due to grain boundary contributions [6]. It is important to notice that very low dielectric constants were observed at high frequency (>100 kHz). Erbil et al. [20] found giant permittivity at low frequency and very low permittivity at higher frequency. We have also observed similar characteristics in relaxor ferroelectric thin films.

Variation of dielectric characteristics with temperature is very important for materials with potential electronic applications. The temperature dependence of real and imaginary permittivities at 10 kHz are shown in Fig. 4a and b. In the temperature range of 100–400 K, the permittivity (ε') exhibited almost constant behavior with small enhancement with increase in temperature. In this temperature range, the dielectric constant decreased (very fast > 100 kHz, above the Debye relaxation) with increase in frequency whereas the tangent loss was much less ($\sim$0.02) at low frequency and increased with increase in frequency. These phenomena are completely new for LNs. Comparable behavior was observed in relaxor ferroelectrics which showed similar frequency dispersion near and below the phase transition temperature. In both cases (LNs and relaxor ferroelectric), frequency dispersion in tangent loss values shifted from low to high frequency with increase in temperature, i.e., low dielectric loss for low frequency and high dielectric loss for higher frequencies [22, 23]. This kind of dielectric behavior ruled out the active participation of space charge in these temperature regions [5, 24]. Above 450 K the reverse phenomenon was observed, i.e., high loss for low frequency, which suggests the possible development of space charge at elevated temperatures.

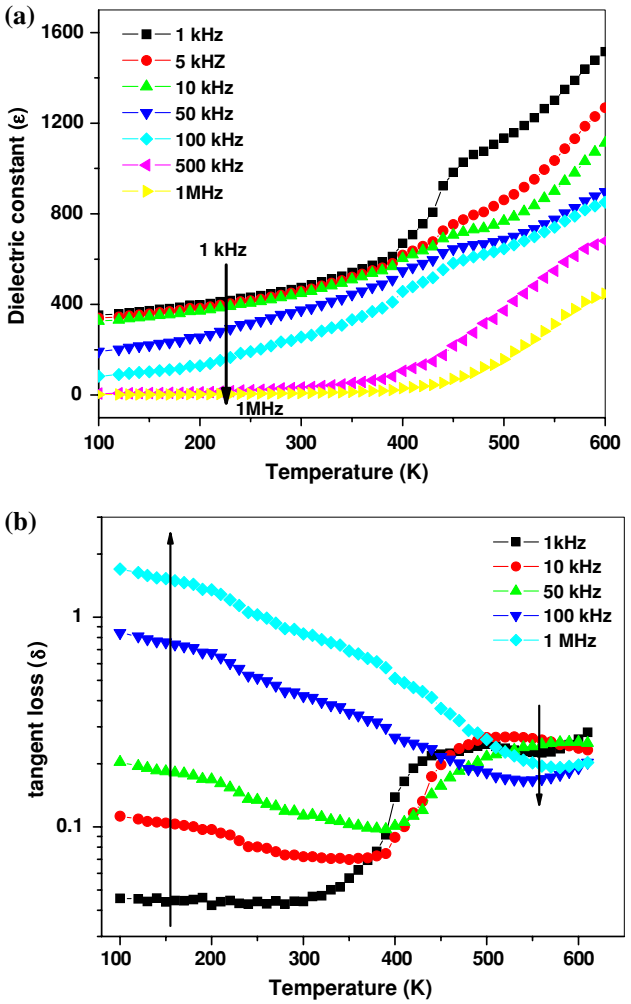

Fig. 4 **a** and **b** Real and imaginary part of permittivity as functions of temperature over wide range of frequencies from 100 Hz to 1 MHz

Room temperature electric field induced polarization switching (P–E) behavior was studied by Sawyer–Tower measurements at 60 Hz. It can be seen from Fig. 5 that LNs thin films have well saturated asymmetric hysteresis loops with remanent polarization (P_r) of about 33 μC/cm^2 for 600 kV/cm maximum external electric field. We did not observe much change in the coercive field with increase in applied electric field. The observed P_r value is comparable with the investigated PZT/$CoFe_2O_4$ multilayer structure [25]. The observed remanent polarization may be attributed to the relaxed local strain, higher nucleation of grains and compositional disorder due to the solid solution of ferroelectric and relaxor at the interfaces. The shift in hysteresis loop observed in LNs on LACO/MgO substrate was about 2–7 V at 250 nm thin films. This hysteresis loop shifted by a similar amount −Ve off set voltage under the application of a DOWN external electric field as shown in Fig. 5. To the best of our knowledge, the ferroelectric imprint has only been attributed to the development of dipole alignment, redistribution of charge carriers under the influence of the depolarization field, and charge injection through the interfacial layer [26, 27]. However, for ferroelectric thin films used in memory applications, only the charge injection through the interfacial layer was found to be compatible with the totality of the experimental observations. The concept employed in this scenario suggests that in the ferroelectric film the polarization decreases gradually within the nearby-interfacial region, and this region is approximated by a low-dielectric-constant layer between the film and the interface. The charge accumulation at the interface is shown to provoke a voltage offset and polarization loss which are nonlinearly dependent on time in a logarithmic scale. This result is obtained for different charge injection mechanisms including Schottky, Pool-Frenkel, and tunneling scenarios.

As we discussed previously, the imprint arising in LNs was not due to the passive layer between substrate and films. PZT films of the same thickness were also grown under the same conditions and did not show any ferroelectric imprint, which indicates imprint arises due to the sandwich structure in the LNs. In present LNs, the ferroelectric PZT slab (∼5 nm) was sandwiched between two multiferroic relaxor (PFW) slabs (∼1 nm). This shows that the imprint is related to the charge injection and charge accumulation in the nearby PFW/PZT/PFW interfaces. A similar ferroelectric hysteresis with similar amount of imprint was observed over a wide range of temperature (100–350 K) (not shown here) with little enhancement in the coercive field at low temperature. As we know, the bi-ferroelectric relaxor PFW possess polar nano regions (PNRs) below 540 K (Burns temperature) whereas these PNRs freeze and form long-range order below temperatures of 150 K (T_f) [9]. The effects of PNRs on ferroelectric hysteresis in LNs are completely new. Careful study is needed to develop theory and models to explain the imprint behavior in ferroelectric-biferroic relaxor nanostructures. A schematic diagram was prepared to explain the blocking phenomena of polarization in LNs (shown in Fig. 5). It indicates that during UP external electric field, the imprint in hysteresis is mainly due to the upper biferroic relaxor regions, whereas in the DOWN electric field the imprint is due to the lower biferroic relaxor regions. XRD analysis indicates that high amounts of tensile strain (∼3.11% along c-axis) were generated along the c-axis near the PZT/PFW interface whereas ∼ −3.21% compressive strain develops along the c-axis near the PFW/PZT interface. Since the LNs possess more than 40 interfaces in the ∼250 nm thin films, we believe a significant amount of internal stress develops in LNs, which may also cause the development of a large amount of imprint in ferroelectric hysteresis. Still a better understanding of imprint in LNs is needed.

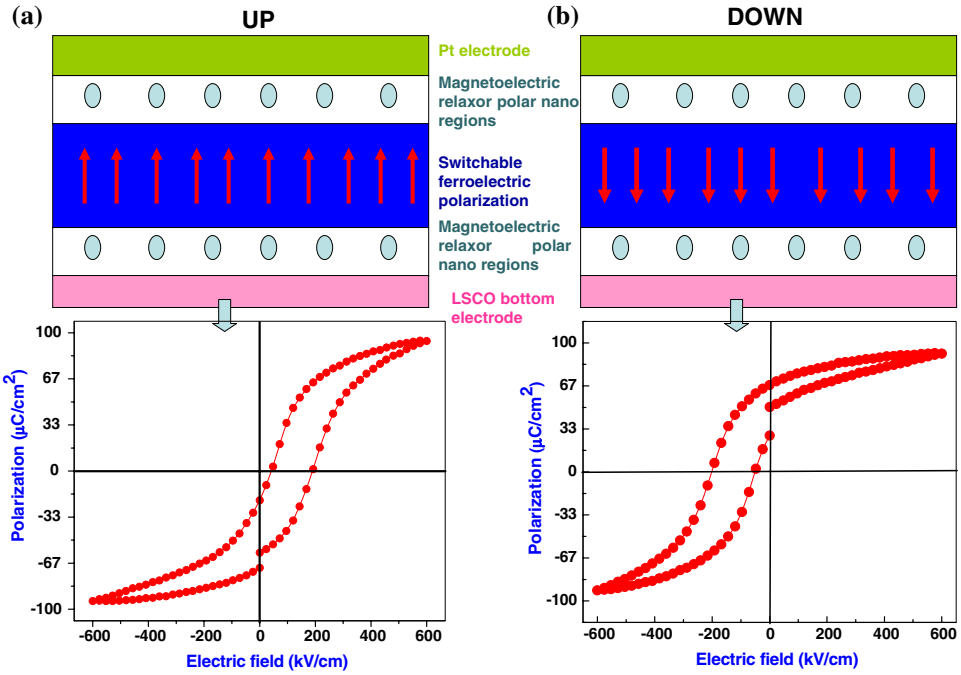

Fig. 5 **a** and **b** Room-temperature electric field induced polarization switching (P–E) for UP and DOWN applied external electric field using Sawyer–Tower measurements at 60 Hz. A model was presented to explain the high imprint in ferroelectric hysteresis

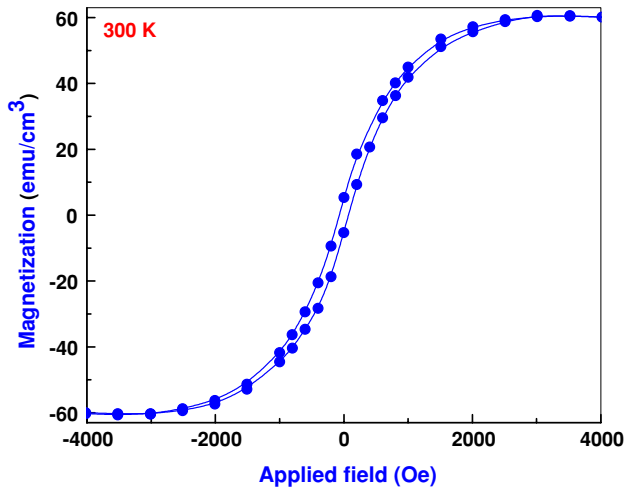

Fig. 6 Magnetization versus applied field (M–H) response of the PZT/PFW LNs thin films at room temperature

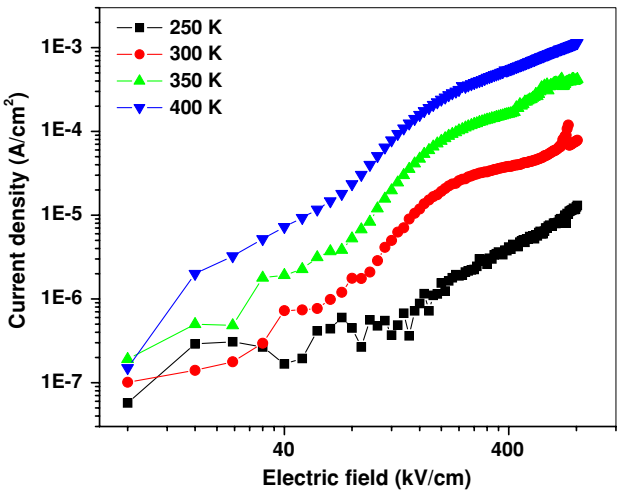

Fig. 7 Current density versus electric field J–E characteristics of epitaxial PZT/PFW LNs thin film measured over wide range of temperature (250–400 K) and electric field (500 kV/cm)

The magnetization versus applied field (M–H) response of the PZT/PFW LNs thin films is shown in Fig. 6, in which the applied magnetic field was parallel to the c-axis. A well saturated ferromagnetic hysteresis was observed with remanent magnetization of 5.32 emu/cc and a coercive field of ~550 Oe under the application of high magnetic fields of ~7 T. M–H data are consistent with previous work on PFW which indicated canted antiferromagnetic (AFM) (~ T_N ~ 343 K) spin order and weak ferromagnetism [10]. As discussed in previous work, a super-exchange in the disordered regions through Fe^{3+}–O–Fe^{3+} is expected to yield antiferromagnetic ordering below the Neel temperature (~ 350 K for PFW) [28]. Usually, angles in the Fe^{3+}–O–Fe^{3+} bonds are close to 180°. The compressive strain in the films may cause a small distortion in the Fe^{3+}–O–Fe^{3+} spins. We believe that the observed room-temperature ferromagnetism is due to spin canting. These LNs possess a great deal of strain (~3.21%) across each PZT/PFW/PZT interface, which might responsible for enhancing ferromagnetism at room temperature.

Figure 7 shows current density vs electric field J–E characteristics of epitaxial PZT/PFW LNs thin films on MgO structures measured over a wide range of temperature (250–400 K). The LNs film shows leakage current densities on the order of 10^{-7} A/cm^2 in the low electric field

region at room temeprature, with an increase (from 10^{-7} A/cm^2 to 10^{-4} A/cm^2) with increasing applied electric field ($\sim$500 kV/cm). The material also shows enhancement in leakage current with increase in temperature. The leakage behavior mechanism may be explained on the basis of different charge injection mechanisms including Schottky, Pool-Frenkel, and tunneling scenarios. Field and temperature dependent measurements showed very low leakage current in the LNs, which provides very high ferroelectric polarization in the layered nanostructure and indicates its suitability for device applications.

There are no published models for imprint in artificially layered ferroelectric superlattices and certainly none for the case in which one set of layers are relaxors. However, it is known [29] that such superlattices have unusually large densities of space charge at their interfaces, and that such charge, injected from the electrodes, exacerbates both fatigue and imprint [30]. In the present case, imprint might be expected to be exaggerated because the bottom electrode (LSCO) and the top electrode (Pt) have different work functions, producing asymmetric charge injection, primarily through the bottom electrode.

In summary, epitaxial ferroelectric PZT and ferroic relaxor PFW layered nanostructures were fabricated on MgO substrate by pulsed laser deposition. These materials showed Debye-type dielectric relaxation over a wide rage of temperature with marked deviation at elevated temperatures, whereas low frequency grain boundary relaxation was observed at elevated temperature. Step-type dielectric behavior with very low dielectric constant above 100 kHz was observed. High dielectric constants with low dielectric loss were seen below 100 kHz and 400 K, similar to relaxor ferroelectrics. Well saturated asymmetric ferroelectric hysteresis loops with high remanent polarization (P_r) of about 33 μC/cm^2 for 600 kV/cm maximum external electric field were found. Ferroelectric hysteresis illustrated high imprint $\sim$5–7 V at 250 nm thin films which may be due to charge accumulation at the interface of layers or significant amount of strain ($\sim$3.21%) along the c-axis of LNs. A well saturated ferromagnetic hysteresis was observed with remanent magnetization 5.32 emu/cc and a coercive field of $\sim$550 Oe. Very low leakage current densities were obtained $\sim 10^{-7} - 10^{-5}$ A/cm^2 at 500 kV/cm. Low leakage current densities, high ferroelectric polarization, well saturated ferromagnetic hysteresis, and flat dielectric constant over wide range of temperature make LNs a potential candidate for artificially designed multiferroics.

Acknowledgements This work was partially supported by DOD W911NF-05-1-0340, W911NF-06-1-0030 and W911NF-06-1-0183 grants.

References

1. Scott JF (2007) Science 315:954
2. Spaldin NA, Fiebig M (2005) Science 309:391
3. Eerenstein W, Mathur ND, Scott JF (2006) Nature 442:759
4. Wang J, Neaton JB, Zheng H, Nagarajan V, Ogale SB, Liu B, Viehland D, Vaithyanathan V, Schlom DG, Waghmare UV, Spaldin NA, Rabe KM, Wuttig M, Ramesh R (2003) Science 299:1719
5. Ortega N, Kumar A, Katiyar RS, Scott JF (2007) Appl Phys Lett 91:102902
6. Ortega N, Kumar A, Bhattacharya P, Majumder SB, Katiyar RS (2008) Phys Rev B 77:014111
7. Zheng H, Wang J, Lo SE, Ma Z, Mohaddes-Ardabili L, Zhao T, Salamanca-Riba L, Shinde SR, Ogale SB, Bai F, Viehland D, Jia Y, Schlom DG, Wuttig M, Roytburd A, Ramesh R (2004) Science 303:661
8. Levstik A, Bobnar V, Filipič C, Holc J, Kosec M, Blinc R, Trontelj Z, Jagličić Z (2007) Appl Phys Lett 91:012905
9. Kumar A, Sharma GL, Katiyar RS, Pirc R, Blinc R, Scott JF (2008) condmat arXiv: 0812.3875v2
10. Kumar A, Rivera I, Katiyar RS, Scott JF (2008) Appl Phys Lett 92:132913
11. Schmid H (1994) Feroelectrics 162:317
12. Ramesh R, Spaldin NA (2007) Nature 6:21
13. Barbosa J, Almeida B, Mendez MA, Rolo AG, Araújo JP (2007) Phys Sat Sol (a) 204:1371
14. Muralidharan R, Dix N, Skumryev V, Varela M, Sanchez F, Fontcuberta J (2008) J Appl Phys 103:07E301
15. Chaudhuri AR, Ranjith R, Krupanidhi SB, Mangalam R, Sundaresan A (2007) Appl Phys Lett 90:122902
16. Li YW, Sun JL, Chen J, Meng XJ, Chu JH (2005) Appl Phys Lett 87:182902
17. Abe K, Komatsu S (1995) J Appl Phys 77:6461
18. Abe K, Komatsu S, Yanase N, Sano K, Kawakubo T (1997) Jpn J Appl Phys 36:5575
19. Abe K, Komatsu S, Yanase N, Sano K, Kawakubo T (1997) Jpn J Appl Phys 36:5846
20. Erbil A, Kim Y, Gerhardt RA (1996) Phys Rev Lett 77:1628
21. Cole KS, Cole RH (1941) J Chem Phys 9:341
22. Correa M, Kumar A, Katiyar RS (2008) J Am Cer Soc 91:1788
23. Correa M, Kumar A, Katiyar RS (2008) Integr Ferroelectr 100:1
24. Catalan G (2006) Appl Phys Lett 88:102902
25. Ortega N, Kumar A, Katiyar RS (2009) Phys Rev B (in press)
26. Warren W, Tuttle B, Dimos D, Pike G, Al-Shareef H, Ramesh R, Evans J (1998) Jpn J Appl Phys Part 1 35:1521
27. Dimos D, Warren W, Sinclair M, Tuttle B, Schwartz R (1994) J Appl Phys 76:4305
28. Ye ZG, Schmid H (1994) Ferroelectrics 162:119
29. Jiang AQ, Scott JF, Dawber M, Wang C (2002) J Appl Phys 92:6756
30. Lou XJ, Zhang M, Redfern SAT, Scott JF (2007) Phys Rev B 75:224104